

# Measurement of the inclusive charmless semileptonic branching fraction of $B$ meson using the full reconstruction tag

K. Abe,<sup>10</sup> K. Abe,<sup>46</sup> N. Abe,<sup>49</sup> I. Adachi,<sup>10</sup> H. Aihara,<sup>48</sup> M. Akatsu,<sup>24</sup> Y. Asano,<sup>53</sup>  
T. Aso,<sup>52</sup> V. Aulchenko,<sup>2</sup> T. Aushev,<sup>14</sup> T. Aziz,<sup>44</sup> S. Bahinipati,<sup>6</sup> A. M. Bakich,<sup>43</sup>  
Y. Ban,<sup>36</sup> M. Barbero,<sup>9</sup> A. Bay,<sup>20</sup> I. Bedny,<sup>2</sup> U. Bitenc,<sup>15</sup> I. Bizjak,<sup>15</sup> S. Blyth,<sup>29</sup>  
A. Bondar,<sup>2</sup> A. Bozek,<sup>30</sup> M. Bračko,<sup>22,15</sup> J. Brodzicka,<sup>30</sup> T. E. Browder,<sup>9</sup> M.-C. Chang,<sup>29</sup>  
P. Chang,<sup>29</sup> Y. Chao,<sup>29</sup> A. Chen,<sup>26</sup> K.-F. Chen,<sup>29</sup> W. T. Chen,<sup>26</sup> B. G. Cheon,<sup>4</sup>  
R. Chistov,<sup>14</sup> S.-K. Choi,<sup>8</sup> Y. Choi,<sup>42</sup> Y. K. Choi,<sup>42</sup> A. Chuvikov,<sup>37</sup> S. Cole,<sup>43</sup>  
M. Danilov,<sup>14</sup> M. Dash,<sup>55</sup> L. Y. Dong,<sup>12</sup> R. Dowd,<sup>23</sup> J. Dragic,<sup>23</sup> A. Drutskoy,<sup>6</sup>  
S. Eidelman,<sup>2</sup> Y. Enari,<sup>24</sup> D. Epifanov,<sup>2</sup> C. W. Everton,<sup>23</sup> F. Fang,<sup>9</sup> S. Fratina,<sup>15</sup>  
H. Fujii,<sup>10</sup> N. Gabyshev,<sup>2</sup> A. Garmash,<sup>37</sup> T. Gershon,<sup>10</sup> A. Go,<sup>26</sup> G. Gokhroo,<sup>44</sup>  
B. Golob,<sup>21,15</sup> M. Grosse Perdekamp,<sup>38</sup> H. Guler,<sup>9</sup> J. Haba,<sup>10</sup> F. Handa,<sup>47</sup> K. Hara,<sup>10</sup>  
T. Hara,<sup>34</sup> N. C. Hastings,<sup>10</sup> K. Hasuko,<sup>38</sup> K. Hayasaka,<sup>24</sup> H. Hayashii,<sup>25</sup> M. Hazumi,<sup>10</sup>  
E. M. Heenan,<sup>23</sup> I. Higuchi,<sup>47</sup> T. Higuchi,<sup>10</sup> L. Hinz,<sup>20</sup> T. Hojo,<sup>34</sup> T. Hokuue,<sup>24</sup>  
Y. Hoshi,<sup>46</sup> K. Hoshina,<sup>51</sup> S. Hou,<sup>26</sup> W.-S. Hou,<sup>29</sup> Y. B. Hsiung,<sup>29</sup> H.-C. Huang,<sup>29</sup>  
T. Igaki,<sup>24</sup> Y. Igarashi,<sup>10</sup> T. Iijima,<sup>24</sup> A. Imoto,<sup>25</sup> K. Inami,<sup>24</sup> A. Ishikawa,<sup>10</sup> H. Ishino,<sup>49</sup>  
K. Itoh,<sup>48</sup> R. Itoh,<sup>10</sup> M. Iwamoto,<sup>3</sup> M. Iwasaki,<sup>48</sup> Y. Iwasaki,<sup>10</sup> R. Kagan,<sup>14</sup> H. Kakuno,<sup>48</sup>  
J. H. Kang,<sup>56</sup> J. S. Kang,<sup>17</sup> P. Kapusta,<sup>30</sup> S. U. Kataoka,<sup>25</sup> N. Katayama,<sup>10</sup> H. Kawai,<sup>3</sup>  
H. Kawai,<sup>48</sup> Y. Kawakami,<sup>24</sup> N. Kawamura,<sup>1</sup> T. Kawasaki,<sup>32</sup> N. Kent,<sup>9</sup> H. R. Khan,<sup>49</sup>  
A. Kibayashi,<sup>49</sup> H. Kichimi,<sup>10</sup> H. J. Kim,<sup>19</sup> H. O. Kim,<sup>42</sup> Hyunwoo Kim,<sup>17</sup> J. H. Kim,<sup>42</sup>  
S. K. Kim,<sup>41</sup> T. H. Kim,<sup>56</sup> K. Kinoshita,<sup>6</sup> P. Koppenburg,<sup>10</sup> S. Korpar,<sup>22,15</sup> P. Krizan,<sup>21,15</sup>  
P. Krokovny,<sup>2</sup> R. Kulasiri,<sup>6</sup> C. C. Kuo,<sup>26</sup> H. Kurashiro,<sup>49</sup> E. Kurihara,<sup>3</sup> A. Kusaka,<sup>48</sup>  
A. Kuzmin,<sup>2</sup> Y.-J. Kwon,<sup>56</sup> J. S. Lange,<sup>7</sup> G. Leder,<sup>13</sup> S. E. Lee,<sup>41</sup> S. H. Lee,<sup>41</sup>  
Y.-J. Lee,<sup>29</sup> T. Lesiak,<sup>30</sup> J. Li,<sup>40</sup> A. Limosani,<sup>23</sup> S.-W. Lin,<sup>29</sup> D. Liventsev,<sup>14</sup>  
J. MacNaughton,<sup>13</sup> G. Majumder,<sup>44</sup> F. Mandl,<sup>13</sup> D. Marlow,<sup>37</sup> T. Matsuishi,<sup>24</sup>  
H. Matsumoto,<sup>32</sup> S. Matsumoto,<sup>5</sup> T. Matsumoto,<sup>50</sup> A. Matyja,<sup>30</sup> Y. Mikami,<sup>47</sup>  
W. Mitaroff,<sup>13</sup> K. Miyabayashi,<sup>25</sup> Y. Miyabayashi,<sup>24</sup> H. Miyake,<sup>34</sup> H. Miyata,<sup>32</sup> R. Mizuk,<sup>14</sup>  
D. Mohapatra,<sup>55</sup> G. R. Moloney,<sup>23</sup> G. F. Moorhead,<sup>23</sup> T. Mori,<sup>49</sup> A. Murakami,<sup>39</sup>  
T. Nagamine,<sup>47</sup> Y. Nagasaka,<sup>11</sup> T. Nakadaira,<sup>48</sup> I. Nakamura,<sup>10</sup> E. Nakano,<sup>33</sup> M. Nakao,<sup>10</sup>  
H. Nakazawa,<sup>10</sup> Z. Natkaniec,<sup>30</sup> K. Neichi,<sup>46</sup> S. Nishida,<sup>10</sup> O. Nitoh,<sup>51</sup> S. Noguchi,<sup>25</sup>  
T. Nozaki,<sup>10</sup> A. Ogawa,<sup>38</sup> S. Ogawa,<sup>45</sup> T. Ohshima,<sup>24</sup> T. Okabe,<sup>24</sup> S. Okuno,<sup>16</sup>  
S. L. Olsen,<sup>9</sup> Y. Onuki,<sup>32</sup> W. Ostrowicz,<sup>30</sup> H. Ozaki,<sup>10</sup> P. Pakhlov,<sup>14</sup> H. Palka,<sup>30</sup>  
C. W. Park,<sup>42</sup> H. Park,<sup>19</sup> K. S. Park,<sup>42</sup> N. Parslow,<sup>43</sup> L. S. Peak,<sup>43</sup> M. Pernicka,<sup>13</sup>  
J.-P. Perroud,<sup>20</sup> M. Peters,<sup>9</sup> L. E. Piilonen,<sup>55</sup> A. Poluektov,<sup>2</sup> F. J. Ronga,<sup>10</sup> N. Root,<sup>2</sup>  
M. Rozanska,<sup>30</sup> H. Sagawa,<sup>10</sup> M. Saigo,<sup>47</sup> S. Saitoh,<sup>10</sup> Y. Sakai,<sup>10</sup> H. Sakamoto,<sup>18</sup>  
T. R. Sarangi,<sup>10</sup> M. Satapathy,<sup>54</sup> N. Sato,<sup>24</sup> O. Schneider,<sup>20</sup> J. Schümann,<sup>29</sup> C. Schwanda,<sup>13</sup>  
A. J. Schwartz,<sup>6</sup> T. Seki,<sup>50</sup> S. Semenov,<sup>14</sup> K. Senyo,<sup>24</sup> Y. Settai,<sup>5</sup> R. Seuster,<sup>9</sup>  
M. E. Sevier,<sup>23</sup> T. Shibata,<sup>32</sup> H. Shibuya,<sup>45</sup> B. Shwartz,<sup>2</sup> V. Sidorov,<sup>2</sup> V. Siegle,<sup>38</sup>  
J. B. Singh,<sup>35</sup> A. Somov,<sup>6</sup> N. Soni,<sup>35</sup> R. Stamen,<sup>10</sup> S. Stanič,<sup>53,\*</sup> M. Starič,<sup>15</sup> A. Sugi,<sup>24</sup>  
A. Sugiyama,<sup>39</sup> K. Sumisawa,<sup>34</sup> T. Sumiyoshi,<sup>50</sup> S. Suzuki,<sup>39</sup> S. Y. Suzuki,<sup>10</sup> O. Tajima,<sup>10</sup>  
F. Takasaki,<sup>10</sup> K. Tamai,<sup>10</sup> N. Tamura,<sup>32</sup> K. Tanabe,<sup>48</sup> M. Tanaka,<sup>10</sup> G. N. Taylor,<sup>23</sup>

Y. Teramoto,<sup>33</sup> X. C. Tian,<sup>36</sup> S. Tokuda,<sup>24</sup> S. N. Tovey,<sup>23</sup> K. Trabelsi,<sup>9</sup> T. Tsuboyama,<sup>10</sup>  
T. Tsukamoto,<sup>10</sup> K. Uchida,<sup>9</sup> S. Uehara,<sup>10</sup> T. Uglov,<sup>14</sup> K. Ueno,<sup>29</sup> Y. Unno,<sup>3</sup> S. Uno,<sup>10</sup>  
Y. Ushiroda,<sup>10</sup> G. Varner,<sup>9</sup> K. E. Varvell,<sup>43</sup> S. Villa,<sup>20</sup> C. C. Wang,<sup>29</sup> C. H. Wang,<sup>28</sup>  
J. G. Wang,<sup>55</sup> M.-Z. Wang,<sup>29</sup> M. Watanabe,<sup>32</sup> Y. Watanabe,<sup>49</sup> L. Widhalm,<sup>13</sup>  
Q. L. Xie,<sup>12</sup> B. D. Yabsley,<sup>55</sup> A. Yamaguchi,<sup>47</sup> H. Yamamoto,<sup>47</sup> S. Yamamoto,<sup>50</sup>  
T. Yamanaka,<sup>34</sup> Y. Yamashita,<sup>31</sup> M. Yamauchi,<sup>10</sup> Heyoung Yang,<sup>41</sup> P. Yeh,<sup>29</sup> J. Ying,<sup>36</sup>  
K. Yoshida,<sup>24</sup> Y. Yuan,<sup>12</sup> Y. Yusa,<sup>47</sup> H. Yuta,<sup>1</sup> S. L. Zang,<sup>12</sup> C. C. Zhang,<sup>12</sup> J. Zhang,<sup>10</sup>  
L. M. Zhang,<sup>40</sup> Z. P. Zhang,<sup>40</sup> V. Zhilich,<sup>2</sup> T. Ziegler,<sup>37</sup> D. Žontar,<sup>21,15</sup> and D. Zürcher<sup>20</sup>

(The Belle Collaboration)

<sup>1</sup>*Aomori University, Aomori*

<sup>2</sup>*Budker Institute of Nuclear Physics, Novosibirsk*

<sup>3</sup>*Chiba University, Chiba*

<sup>4</sup>*Chonnam National University, Kwangju*

<sup>5</sup>*Chuo University, Tokyo*

<sup>6</sup>*University of Cincinnati, Cincinnati, Ohio 45221*

<sup>7</sup>*University of Frankfurt, Frankfurt*

<sup>8</sup>*Gyeongsang National University, Chinju*

<sup>9</sup>*University of Hawaii, Honolulu, Hawaii 96822*

<sup>10</sup>*High Energy Accelerator Research Organization (KEK), Tsukuba*

<sup>11</sup>*Hiroshima Institute of Technology, Hiroshima*

<sup>12</sup>*Institute of High Energy Physics,*

*Chinese Academy of Sciences, Beijing*

<sup>13</sup>*Institute of High Energy Physics, Vienna*

<sup>14</sup>*Institute for Theoretical and Experimental Physics, Moscow*

<sup>15</sup>*J. Stefan Institute, Ljubljana*

<sup>16</sup>*Kanagawa University, Yokohama*

<sup>17</sup>*Korea University, Seoul*

<sup>18</sup>*Kyoto University, Kyoto*

<sup>19</sup>*Kyungpook National University, Taegu*

<sup>20</sup>*Swiss Federal Institute of Technology of Lausanne, EPFL, Lausanne*

<sup>21</sup>*University of Ljubljana, Ljubljana*

<sup>22</sup>*University of Maribor, Maribor*

<sup>23</sup>*University of Melbourne, Victoria*

<sup>24</sup>*Nagoya University, Nagoya*

<sup>25</sup>*Nara Women's University, Nara*

<sup>26</sup>*National Central University, Chung-li*

<sup>27</sup>*National Kaohsiung Normal University, Kaohsiung*

<sup>28</sup>*National United University, Miao Li*

<sup>29</sup>*Department of Physics, National Taiwan University, Taipei*

<sup>30</sup>*H. Niewodniczanski Institute of Nuclear Physics, Krakow*

<sup>31</sup>*Nihon Dental College, Niigata*

<sup>32</sup>*Niigata University, Niigata*

<sup>33</sup>*Osaka City University, Osaka*

<sup>34</sup>*Osaka University, Osaka*

<sup>35</sup>*Panjab University, Chandigarh*

<sup>36</sup>*Peking University, Beijing*

- <sup>37</sup>*Princeton University, Princeton, New Jersey 08545*  
<sup>38</sup>*RIKEN BNL Research Center, Upton, New York 11973*  
<sup>39</sup>*Saga University, Saga*  
<sup>40</sup>*University of Science and Technology of China, Hefei*  
<sup>41</sup>*Seoul National University, Seoul*  
<sup>42</sup>*Sungkyunkwan University, Suwon*  
<sup>43</sup>*University of Sydney, Sydney NSW*  
<sup>44</sup>*Tata Institute of Fundamental Research, Bombay*  
<sup>45</sup>*Toho University, Funabashi*  
<sup>46</sup>*Tohoku Gakuin University, Tagajo*  
<sup>47</sup>*Tohoku University, Sendai*  
<sup>48</sup>*Department of Physics, University of Tokyo, Tokyo*  
<sup>49</sup>*Tokyo Institute of Technology, Tokyo*  
<sup>50</sup>*Tokyo Metropolitan University, Tokyo*  
<sup>51</sup>*Tokyo University of Agriculture and Technology, Tokyo*  
<sup>52</sup>*Toyama National College of Maritime Technology, Toyama*  
<sup>53</sup>*University of Tsukuba, Tsukuba*  
<sup>54</sup>*Utkal University, Bhubaneswer*  
<sup>55</sup>*Virginia Polytechnic Institute and State University, Blacksburg, Virginia 24061*  
<sup>56</sup>*Yonsei University, Seoul*

## Abstract

We present a preliminary measurement of the inclusive charmless semileptonic branching fraction of the  $B$  meson, based on  $140 \text{ fb}^{-1}$  of data collected by the Belle detector at the KEKB  $e^+e^-$  asymmetric collider. Events are tagged by fully reconstructing one of the  $B$  mesons, produced in pairs from  $\Upsilon(4S)$ . The signal for  $b \rightarrow u$  semileptonic decay is distinguished from the  $b \rightarrow c$  semileptonic background using the hadronic and leptonic invariant mass distributions  $M_X$  and  $q^2$ . We find the partial branching fraction for the kinematical region given by  $M_X < 1.7 \text{ GeV}/c^2$  and  $q^2 > 8 \text{ GeV}^2/c^2$ ,  $\Delta\mathcal{B}(B \rightarrow X_u\ell\nu) = [0.99 \pm 0.15(\text{stat}) \pm 0.18(\text{syst}) \pm 0.04(b \rightarrow u) \pm 0.07(b \rightarrow c)] \times 10^{-3}$ . Using a theoretical prediction for the extrapolation to the full range of  $M_X$  and  $q^2$  variables, we obtain  $\mathcal{B}(B \rightarrow X_u\ell\nu) = [3.37 \pm 0.50(\text{stat}) \pm 0.60(\text{syst}) \pm 0.14(b \rightarrow u) \pm 0.24(b \rightarrow c) \pm 0.50(f_u \text{ error})] \times 10^{-3}$ . From this measurement, the magnitude of the Cabibbo-Kobayashi-Maskawa matrix element  $V_{ub}$  is  $|V_{ub}| = [5.54 \pm 0.42(\text{stat}) \pm 0.50(\text{syst}) \pm 0.12(b \rightarrow u) \pm 0.19(b \rightarrow c) \pm 0.42(f_u \text{ error}) \pm 0.27(\mathcal{B} \rightarrow |V_{ub}| \text{ error})] \times 10^{-3}$ .

PACS numbers: 12.15.Hh, 11.30.Er, 13.25.Hw

## INTRODUCTION

Measurement of the Cabibbo-Kobayashi-Maskawa matrix element  $|V_{ub}|$  is crucial to test the Standard Model prediction of  $CP$  violation. In this paper, we report a preliminary measurement of the inclusive charmless semileptonic branching fraction of the  $B$  meson  $\mathcal{B}(B \rightarrow X_u \ell \nu)$ , which provides one of the best ways to determine  $|V_{ub}|$ . In this measurement, one of the  $B$  mesons, referred to as the tag side meson,  $B_{\text{tag}}$ , is fully reconstructed in several hadronic decay modes to tag the production, flavor and charge as well as the momentum of the  $B$  meson. The semileptonic decay of the other  $B$  meson, referred to as the signal side meson,  $B_{\text{sig}}$ , is detected by the presence of a high momentum electron or muon. This method allows one to reconstruct the invariant mass of the hadronic system in the semileptonic decay,  $M_X$ . The invariant mass squared of the leptonic system,  $q^2$ , can also be determined by inferring the missing neutrino momentum. Both kinematical quantities are used to separate the  $B \rightarrow X_u \ell \nu$  signal decays from the abundant  $B \rightarrow X_c \ell \nu$  background decays, with a good signal-to-noise ratio. A similar type of analysis was performed by BaBar, where only a cut on  $M_X$  was applied [1]. According to a recent theoretical calculation [2], a simultaneous cut on the two variables is beneficial because it reduces theoretical uncertainties. Such a simultaneous cut on the two variables was used in a similar analysis by Belle where, instead of the full reconstruction tagging, a simulated annealing technique was applied to separate the two  $B$  meson decays [3].

This measurement has an advantage over the measurements based on the lepton momentum alone [4] in that it covers a relatively large phase space of the signal spectrum, which reduces the error in extrapolating the measured partial branching fraction to obtain the total branching fraction. While the method has these unique features, it requires a large sample of  $B\bar{B}$  events because the full reconstruction efficiency is rather low, typically of the order of 0.3%.

The data used in the present analysis were collected with the Belle detector at the asymmetric energy KEKB [5] storage ring. The Belle detector [6] is a large-solid-angle magnetic spectrometer that consists of a three-layer silicon vertex detector (SVD), a 50-layer central drift chamber (CDC), an array of aerogel threshold Čerenkov counters (ACC), a barrel-like arrangement of time-of-flight scintillation counters (TOF), and an electromagnetic calorimeter (ECL) comprised of CsI(Tl) crystals located inside a super-conducting solenoid coil that provides a 1.5 T magnetic field. An iron flux-return located outside of the coil is instrumented to detect  $K_L^0$  mesons and to identify muons (KLM).

The result presented in this paper is based on a  $140 \text{ fb}^{-1}$  data sample recorded at the  $\Upsilon(4S)$  resonance, which contains  $152 \times 10^6 B\bar{B}$  pairs. An additional  $15 \text{ fb}^{-1}$  data sample taken at a center-of-mass energy 60 MeV below the  $\Upsilon(4S)$  resonance is used to subtract the background from the  $e^+e^- \rightarrow q\bar{q}$  process ( $q = u, d, s, c$ ).

Monte Carlo simulated events were used to determine the efficiency as well as signal and background distributions in the control variables. The simulation program is based on GEANT [7] and fully describes the detector geometry and response. To model the  $B \rightarrow X_u \ell \nu$  decays, we employ a combination of exclusive channels, where  $X_u$  is either a  $\pi$  or a  $\rho$  [8] or an excited  $X_u$  state [9], and an inclusive model for non-resonant final states [10]. The  $B \rightarrow X_c \ell \nu$  transitions are simulated according to the QQ decay generator [11].

This paper is organized as follows. We first discuss the reconstruction of the tag side  $B$  meson, requirements on the signal side and the signal yield extraction. The observed number of  $B \rightarrow X_u \ell \nu$  decays is then converted into a partial branching fraction for the

kinematical region given by  $M_X < 1.7 \text{ GeV}/c^2$  and  $q^2 > 8 \text{ GeV}^2/c^2$ , for which the theoretical uncertainties in modeling  $b \rightarrow u$  transitions are small. The theoretical result [2] quoted above together with the  $b$ -quark shape function parameters determined from the Belle  $b \rightarrow s\gamma$  measurement [12] is used to extract the branching fraction for charmless semileptonic decays, which is, finally, used to obtain the magnitude of the  $V_{ub}$  matrix element.

## RECONSTRUCTION OF THE TAGGING SIDE

In the present analysis,  $B_{\text{tag}}$  candidates are reconstructed in the decay modes,  $B^0 \rightarrow D^{(*)-}\pi^+/\rho^+/a_1^+/D_s^{(*)+}$  and  $B^+ \rightarrow \bar{D}^{(*)0}\pi^+/\rho^+/a_1^+/D_s^{(*)+}$ . Inclusion of charge conjugate decays is implied throughout this paper.

Primary charged tracks are reconstructed with hit information from the CDC. They are required to satisfy track quality cuts based on their impact parameters relative to the measured profile of the interaction point of the two beams.

Charged kaons are identified combining specific ionization ( $dE/dx$ ) measurements in the CDC, Čerenkov light yields in the ACC and time-of-flight measurements in the TOF. The kaon identification efficiency is approximately 88% and the average pion fake rate is about 8%.

Candidate  $\pi^0$  mesons are reconstructed using  $\gamma\gamma$  pairs with an invariant mass between 117.8 and 150.2 MeV/ $c^2$ . Each photon is required to have a minimum energy deposit of  $E_\gamma \geq 50 \text{ MeV}$  ( $E_\gamma \geq 30 \text{ MeV}$  for neutral pions from  $D^*$  decays).

$K_S^0$  mesons are reconstructed using pairs of charged tracks that have an invariant mass within  $\pm 30 \text{ MeV}/c^2$  of the known  $K_S^0$  mass and a well reconstructed vertex that is displaced from the interaction point. Candidate  $\rho^+$  and  $\rho^0$  mesons are reconstructed in the decay modes  $\pi^+\pi^0$  and  $\pi^+\pi^-$ , by requiring their invariant mass to be within  $\pm 225 \text{ MeV}/c^2$  of the nominal  $\rho$  mass. Then,  $a_1^+$  candidates are selected by combining a  $\rho^0$  candidate and a pion, if their invariant mass lies between 0.7 and 1.6 GeV/ $c^2$  and if the three tracks form a good vertex.

$\bar{D}^0$  candidates are reconstructed in the  $\bar{D}^0 \rightarrow K^+\pi^-$ ,  $K^+\pi^-\pi^0$ ,  $K^+\pi^+\pi^-\pi^-$ ,  $K_S^0\pi^0$ ,  $K_S^0\pi^+\pi^-$ ,  $K_S^0\pi^+\pi^-\pi^0$  and  $K^+K^-$  decay modes, while  $D^-$  candidates are reconstructed in the  $D^- \rightarrow K^+\pi^-\pi^-$ ,  $K^+\pi^-\pi^-\pi^0$ ,  $K_S^0\pi^-$ ,  $K_S^0\pi^-\pi^0$ ,  $K_S^0\pi^-\pi^-\pi^+$  and  $K^+K^-\pi^-$  decays.  $D_s^+$  candidates are reconstructed in the decay modes  $D_s^+ \rightarrow K_S^0K^+$  and  $K^+K^-\pi^+$ . These candidates are required to have an invariant mass  $m_D$  within  $\pm 4-5\sigma$  of the nominal  $D$  mass, where the mass resolution  $\sigma$  depends on the decay mode.  $\bar{D}^*$  mesons are reconstructed by combining the  $\bar{D}$  candidate and a low momentum pion,  $D^{*-} \rightarrow \bar{D}^0\pi^-/D^-\pi^0$  and  $\bar{D}^{*0} \rightarrow \bar{D}^0\pi^0$ . They are required to have a mass difference  $\Delta m = m_{\bar{D}\pi} - m_{\bar{D}}$  within  $\pm 5 \text{ MeV}/c^2$  ( $\pm 4-6\sigma$ ) of the nominal value. For the decays with a photon,  $\bar{D}^{*0} \rightarrow \bar{D}^0\gamma$  and  $D_s^{*+} \rightarrow D_s^+\gamma$ , we require that the mass difference  $\Delta m = m_{\bar{D}\gamma} - m_{\bar{D}}$  be within  $\pm 20 \text{ MeV}/c^2$  ( $\pm 2\sigma$ ) of the nominal value.

The selection of  $B_{\text{tag}}$  candidates is based on the beam-constrained mass,  $M_{\text{bc}} = \sqrt{E_{\text{beam}}^{*2}/c^4 - p_B^{*2}/c^2}$ , and the energy difference,  $\Delta E = E_B^* - E_{\text{beam}}^*$ . Here  $E_{\text{beam}}^* = \sqrt{s}/2 \simeq 5.290 \text{ GeV}$  is the beam energy in the center of mass system, and  $p_B^*$  and  $E_B^*$  are the cms momentum and energy of the reconstructed  $B$  meson. (Throughout this paper the variables calculated in the center of mass system will be denoted with an asterisk.) Events satisfying  $M_{\text{bc}} \geq 5.22 \text{ GeV}/c^2$  and  $|\Delta E| \leq 0.3 \text{ GeV}$  are subject to further analysis.

The combinatorial background from jet-like  $e^+e^- \rightarrow q\bar{q}$  processes is suppressed by event

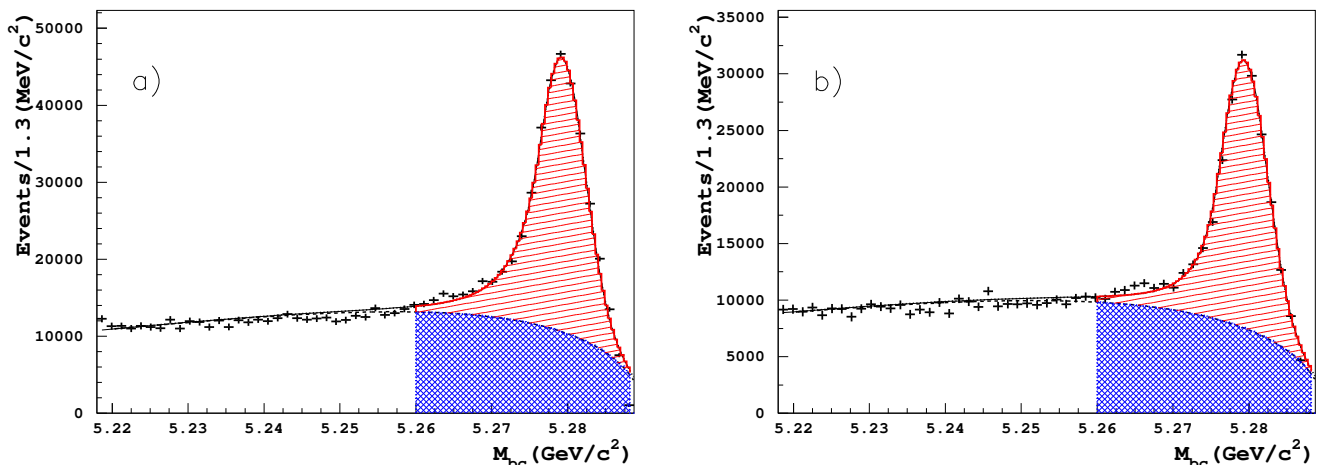


FIG. 1: Beam-constrained mass ( $M_{bc}$ ) distribution for the  $B^+$ (a) and  $B^0$ (b) candidates with the  $-0.2 \text{ GeV} < \Delta E < 0.05 \text{ GeV}$  requirement. The scaled distribution of off-resonance data is subtracted. The shaded areas indicate the results of the fit in the  $M_{bc}$  signal region.

topology cuts based on the normalized second Fox-Wolfram moment ( $R_2$ ) [13],  $R_2 < 0.5$ , and for some modes also by a cut on  $|\cos \theta_{\text{thrust}}| < 0.8$ , where  $\theta_{\text{thrust}}$  is the angle between the thrust axis of the  $B$  candidate and that of the rest of the event.

The signal region for the tagging  $B$  is defined with the cuts  $M_{bc} \geq 5.26 \text{ GeV}/c^2$  and  $-0.2 \text{ GeV} < \Delta E < 0.05 \text{ GeV}$ . The cuts are optimized to maximize the statistics of the signal, while minimizing the migration of tracks between the tag and signal sides.

If an event has multiple  $B_{\text{tag}}$  candidates, we choose the candidate having the smallest  $\chi^2$  based on the deviations from the nominal values of  $\Delta E$ ,  $m_D$ , and  $\Delta m$  if applicable.

Figure 1 shows the distribution of  $M_{bc}$  for the  $B^0$  and  $B^+$  candidates in the  $\Delta E$  signal region. The  $q\bar{q}$  background contribution is subtracted using the scaled off-resonance data. The numbers of tagged events are estimated to be  $(1.58 \pm 0.18) \times 10^5$  for  $B^0$  and  $(2.47 \pm 0.22) \times 10^5$  for  $B^+$ , by fitting the distribution with empirical signal [14] and background functions [15]. The reconstruction efficiencies are 0.21% and 0.33%, while the purities are 47% and 50% for the  $B^0$  and  $B^+$  samples, as determined using scaled off-resonance data subtraction.

## RECONSTRUCTION OF THE SIGNAL SIDE

For events tagged by fully reconstructed  $B_{\text{tag}}$  candidates, we search for electrons or muons from semileptonic decays of the signal side  $B$  meson. Electron identification is based on a combination of the  $dE/dx$  value as measured in the CDC, the response of the ACC, the shower shape in the ECL and the ratio of the energy deposit in the ECL to the momentum measured by the tracking system. Muon identification by the KLM relies on the number of hits in resistive plate counters interspersed in the iron yoke. The lepton identification efficiencies are about 90% for both electrons and muons in the momentum region above  $1 \text{ GeV}/c$ . The hadron fake rate is measured using  $K_S^0 \rightarrow \pi^+\pi^-$  and  $\phi^0 \rightarrow K^+K^-$  decays, and found to be less than 0.2% for electrons and 1.5% for muons in the same momentum region.

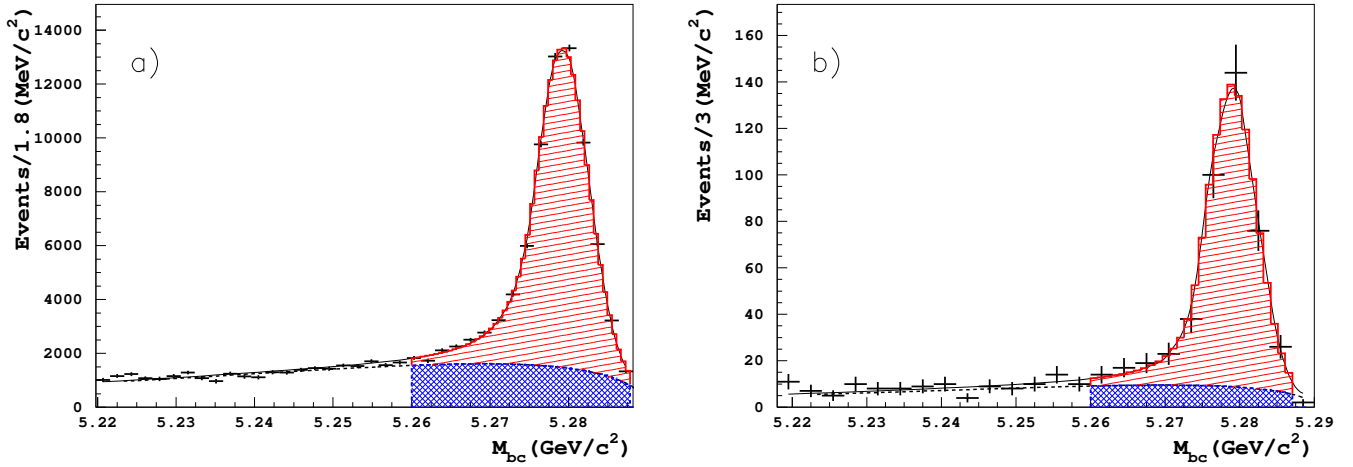


FIG. 2: Beam-constrained mass ( $M_{bc}$ ) distribution for prompt semileptonic decays (a) and events satisfying all  $B \rightarrow X_u l \nu$  signal requirements, including  $M_X < 1.7$  GeV/c<sup>2</sup> and  $q^2 > 8$  GeV<sup>2</sup>/c<sup>2</sup> (b). The shaded areas indicate the results of the fit in the  $M_{bc}$  signal region.

We select electrons having  $p^* \geq 0.6$  GeV/c and  $p_t \geq 0.6$  GeV/c, and muons with  $p_\mu^* \geq 0.8$  GeV/c and  $p_t \geq 0.7$  GeV/c, with  $p_t$  being the transverse momentum component with respect to the positron beam axis. We also require that they are detected in the laboratory polar angular region of  $26^\circ \leq \theta \leq 140^\circ$ . Backgrounds from  $J/\psi$  decays, photon conversions in the material of the detector and  $\pi^0$  Dalitz decays are minimized by imposing veto conditions; we calculate invariant masses for each lepton candidate when combined with opposite charge leptons ( $m_{\ell\ell}$ ) and with an additional photon in the case of electrons ( $m_{ee\gamma}$ ), and reject the lepton if  $m_{\ell\ell}$  lies within  $\pm 5\sigma$  of the nominal  $J/\psi$  mass,  $m_{ee}$  within  $\pm 100$  MeV/c<sup>2</sup> or  $m_{ee\gamma}$  within  $\pm 3\sigma$  of the nominal  $\pi^0$  mass.

For the prompt semileptonic decay signal, we require a lepton with momentum  $p^*$  exceeding 1 GeV/c. We also require the lepton charge to be consistent with a prompt semileptonic decay, when the  $B_{\text{tag}}$  candidate is charged. No requirement is imposed on the lepton charge when the  $B_{\text{tag}}$  candidate is neutral.

The  $B \rightarrow X_u l \nu$  signal events are selected by imposing several requirements to suppress the  $B \rightarrow X_c l \nu$  background as well as the background from poorly reconstructed events. Fake charged tracks, arising mainly from duplication in the tracking of low momentum curling tracks, are removed on the basis of the angle between the two track candidates, and the difference in their momenta. We require that the event contains only one lepton, has zero net charge ( $\sum_i Q_i = 0$ ) and has a missing mass consistent with zero ( $-1 \text{ GeV}^2/c^4 \leq m_{\text{miss}}^2 \leq 0.5 \text{ GeV}^2/c^4$ ). In order to further suppress the  $B \rightarrow X_c l \nu$  background, we require that the number of kaons, either  $K^\pm$  or  $K_S^0$ , is zero ( $N_K = 0$ ) on the signal side. To reject events containing a  $K_L$  meson, we require that the angle between the missing momentum and the direction of the candidate  $K_L$  cluster be greater than  $37^\circ$ .

Finally, we select the signal events with requirements on the invariant mass of the hadronic system  $M_X$  and invariant mass squared of the leptonic system  $q^2$ . The variable  $M_X$  is calculated from the measured momenta of all charged tracks and energy deposits of all neutral clusters in the ECL that are not used in the  $B_{\text{tag}}$  reconstruction or not identified as leptons. Charged tracks are assigned the mass of the pion, kaon or proton, based on the

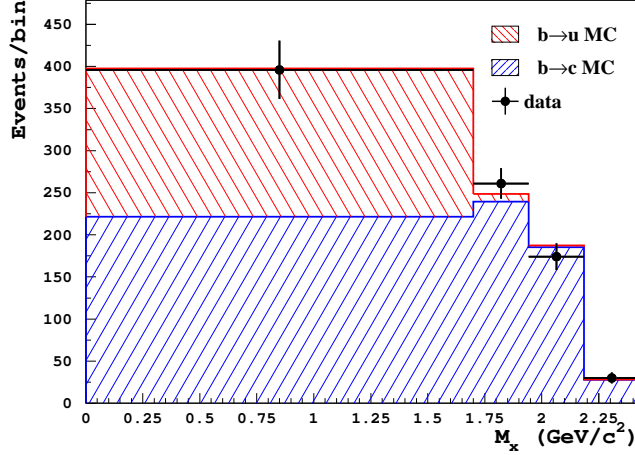


FIG. 3:  $M_X$  distribution for the selected events with  $q^2 > 8 \text{ GeV}^2/c^2$ , data and fitted contributions of the  $B \rightarrow X_c \ell \nu$  and  $B \rightarrow X_u \ell \nu$  transitions.

information from the particle identification system. According to Monte Carlo simulations the resolution in  $M_X$  for the selected events is found to be about  $125 \text{ MeV}/c^2$  and  $130 \text{ MeV}/c^2$  for  $B \rightarrow X_u \ell \nu$  and  $B \rightarrow X_c \ell \nu$  processes, respectively. The four-momentum transfer  $q$  is calculated as  $q = p_{\Upsilon(4S)} - p_{B_{\text{tag}}} - p_X$ , where  $p_{\Upsilon(4S)}$ ,  $p_{B_{\text{tag}}}$  and  $p_X$  are the four-momentum vectors of the  $\Upsilon(4S)$ ,  $B_{\text{tag}}$  and the reconstructed hadronic system, respectively.

Our signal region is defined as  $M_X < 1.7 \text{ GeV}/c^2$  and  $q^2 > 8 \text{ GeV}^2/c^2$ . With these requirements, we suppress the kinematic region where the theoretical interpretation of the result would be difficult [2], and also reduce the level of the  $B \rightarrow X_c \ell \nu$  background. The distribution in the beam constrained mass for the selected events is shown in Fig. 2(b).

## SIGNAL YIELD EXTRACTION

The signal yield is extracted by a fit to the distribution of hadronic invariant mass  $M_X$  for the selected events with  $q^2 > 8 \text{ GeV}^2/c^2$ . The distribution of events in hadronic mass is determined by dividing the data into several  $M_X$  bins. For each bin, the yield is extracted from a fit with empirical signal [14] and background functions [15] to the corresponding  $M_{bc}$  distribution, an example of which is shown in Fig. 2(b). Figure 3 shows the resulting  $M_X$  distribution.

To determine the raw number of events corresponding to the  $B \rightarrow X_u \ell \nu$  process, we first fit the  $M_X$  distribution with two contributions, the signal and the background from the  $B \rightarrow X_c \ell \nu$  process. The shapes of both contributions are determined from Monte Carlo simulation. The result of the fit is indicated in Fig. 3. Using the same relative normalization of the processes, we plot in Figs. 4 and 5 the distributions of events over the  $M_X$  (finer granularity as compared to Fig. 3) and  $q^2$  variables. In the regions of low  $M_X$  ( $< 1.7 \text{ GeV}/c^2$ ) and high  $q^2$  a clear contribution from  $B \rightarrow X_u \ell \nu$  can be observed.

The raw yield of  $B \rightarrow X_u \ell \nu$  decay in the signal region,  $N_{b \rightarrow u}^{\text{raw}} = 174 \pm 26$ , is determined by subtracting the fitted  $B \rightarrow X_c \ell \nu$  contribution (Fig. 3). The error is statistical only.

In order to extract the partial branching fraction  $\Delta\mathcal{B}$  for  $B \rightarrow X_u \ell \nu$  in the signal region  $M_X < 1.7 \text{ GeV}/c^2$ ,  $q^2 > 8 \text{ GeV}^2/c^2$ , Monte Carlo simulation is used to convert the observed



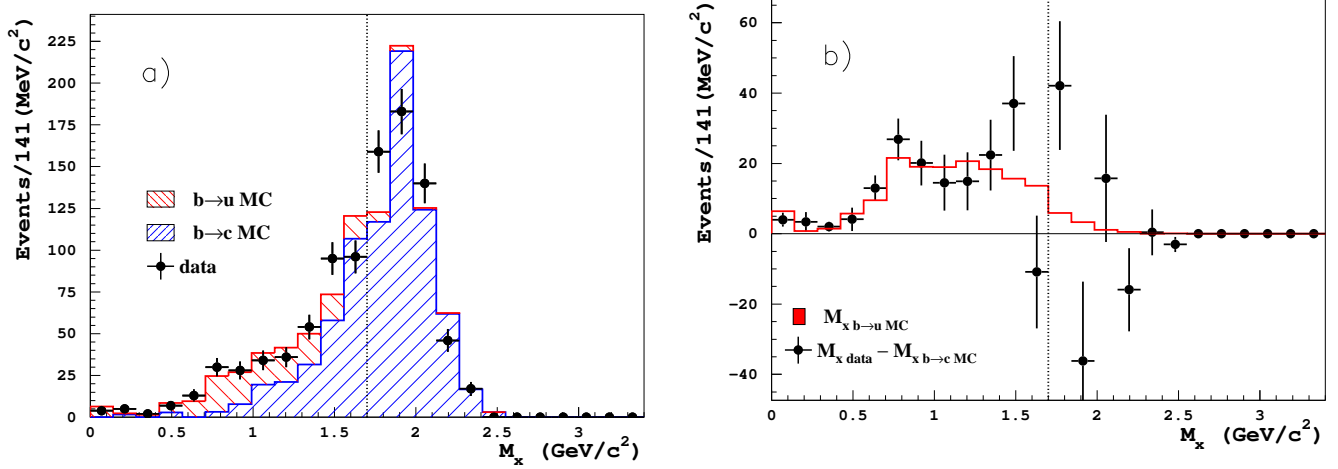


FIG. 4:  $M_X$  distributions for the selected events with  $q^2 > 8 \text{ GeV}^2/c^2$ : a) data and fitted contributions of the  $B \rightarrow X_c \ell \nu$  and  $B \rightarrow X_u \ell \nu$  transitions, b) measured distribution for the  $B \rightarrow X_u \ell \nu$  transition, obtained by subtracting the fitted  $B \rightarrow X_c \ell \nu$  contribution from the data, compared to the simulated  $B \rightarrow X_u \ell \nu$  contribution with the normalization given by the fit. The final cut on  $M_X$  is indicated by a dotted line.

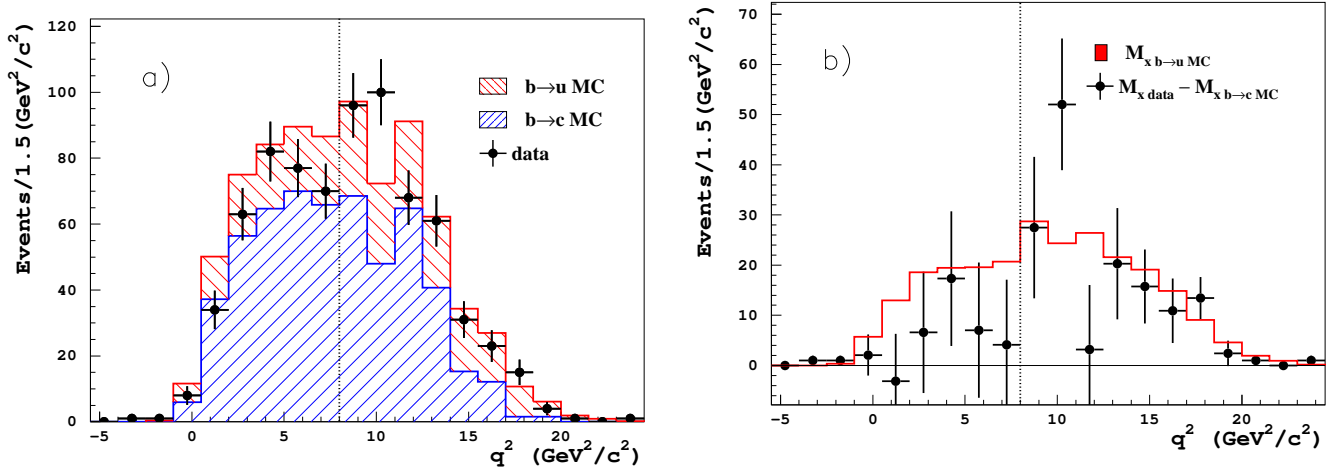


FIG. 5: The  $q^2$  distribution for the selected events with  $M_X < 1.7 \text{ GeV}/c^2$ : a) data and contributions of the  $B \rightarrow X_c \ell \nu$  and  $B \rightarrow X_u \ell \nu$  transitions, normalized with the fit to the  $M_X$  distribution, b) measured distribution for the  $B \rightarrow X_u \ell \nu$  transition, obtained by subtracting the  $B \rightarrow X_c \ell \nu$  contribution from the data, compared to the simulated  $B \rightarrow X_u \ell \nu$  contribution. The final cut on  $q^2$  is indicated by a dotted line.

number of events  $N_{b \rightarrow u}^{\text{raw}}$  to the true number of signal events produced in this region,  $N_{b \rightarrow u}$ , and to estimate the efficiency for these events to be observed anywhere.  $N_{b \rightarrow u}$  is estimated by  $N_{b \rightarrow u} = N_{b \rightarrow u}^{\text{raw}} \times F$ , with  $F = 1 + N_2/N_1 - N_3/N_1$ . Here  $N_1$  is the number of simulated events observed in the signal region and  $N_2$  ( $N_3$ ) is the number of events generated inside (outside) the signal region and observed outside (inside) the signal region. We find  $F = 0.984 \pm 0.014$ ,

and thus  $N_{b \rightarrow u} = 171 \pm 26$ . The efficiency  $\epsilon_{\text{sel}}^{b \rightarrow u}$  for selecting  $B \rightarrow X_u \ell \nu$  events after the lepton momentum cut is predicted to be 27.4%.

The relative partial branching fraction  $\Delta\mathcal{B}(B \rightarrow X_u \ell \nu)/\mathcal{B}(B \rightarrow X \ell \nu)$  is obtained by

$$\frac{\Delta\mathcal{B}(B \rightarrow X_u \ell \nu)}{\mathcal{B}(B \rightarrow X \ell \nu)} = \frac{N_{b \rightarrow u}}{N_{\text{sl}}} \times \frac{1}{\epsilon_{\text{sel}}^{b \rightarrow u}} \times \frac{\epsilon_{\text{frec}}^{\text{sl}}}{\epsilon_{\text{frec}}^{b \rightarrow u}} \times \frac{\epsilon_l^{\text{sl}}}{\epsilon_l^{b \rightarrow u}} \quad . \quad (1)$$

Here  $N_{\text{sl}} = (5.07 \pm 0.04) \times 10^4$  is the number of events having at least one lepton with  $p^* \geq 1.0 \text{ GeV}/c$ , determined from a fit to the corresponding  $M_{\text{bc}}$  distribution (Fig. 2(a)), and corrected for the expected fraction of background events from non-semileptonic decays (14.1%), as estimated by MC simulation. The factor  $\epsilon_{\text{frec}}^{\text{sl}}/\epsilon_{\text{frec}}^{b \rightarrow u}$  accounts for a possible difference in the  $B_{\text{tag}}$  reconstruction efficiency in the presence of a semileptonic or  $B \rightarrow X_u \ell \nu$  decay;  $\epsilon_l^{\text{sl}}/\epsilon_l^{b \rightarrow u}$  is the ratio of fractions of semileptonic decay leptons with  $p^* > 1 \text{ GeV}/c$ , in the whole phase space for the  $B \rightarrow X_c \ell \nu$  events, and within the region  $M_X < 1.7 \text{ GeV}/c^2$  and  $q^2 > 8 \text{ GeV}^2/c^2$  for signal events. The product of efficiency ratios is found to be  $\epsilon_{\text{frec}}^{\text{sl}}/\epsilon_{\text{frec}}^{b \rightarrow u} \times \epsilon_l^{\text{sl}}/\epsilon_l^{b \rightarrow u} = 0.75 \pm 0.048$ .

## SYSTEMATIC ERRORS

The major sources of systematic error in the relative branching fraction are the uncertainty in the background subtraction to extract the yield  $N_{b \rightarrow u}$ , the uncertainties in the calculation of the efficiency ratios, and the uncertainty due to the treatment of  $B \rightarrow X_u \ell \nu$  decays in the Monte Carlo simulation that is used to estimate  $\epsilon_{\text{sel}}^{b \rightarrow u}$  and  $F$ .

The validity of the  $B \rightarrow X_c \ell \nu$  background simulation is tested with the  $B \rightarrow X_c \ell \nu$  enhanced control sample, where all selection cuts are applied with one exception: we require at least one kaon in the event. We have checked that for the  $M_X$  distribution of this control sample there is good agreement between data and the simulation. The relative errors arising from uncertainties in the background subtraction to extract  $N_{b \rightarrow u}$  are estimated to be 7% due to the uncertainty in the modeling of the  $B \rightarrow X_c \ell \nu$  background and 15% due to the limited statistics for the simulated background events.

Statistical uncertainty in the determination of efficiency ratios contributes 6% to the systematic error. The uncertainty in the ratio  $F/\epsilon_{\text{sel}}^{b \rightarrow u}$  is estimated by varying the parameters of the simulation model for  $B \rightarrow X_u \ell \nu$  decays. We assign a 4% error after varying the parameters of the inclusive model within their errors.

The uncertainties due to systematic errors in tracking efficiency, particle identification efficiency and cluster finding efficiency are estimated by varying them by their respective errors, and observing the effect on the value of partial branching fraction. These sources give correlated errors on simulated  $b \rightarrow u$  and  $b \rightarrow c$  events so we add or subtract the error of each source linearly for the two samples, according to the relative sign of their effect. The contributions for different sources are combined in quadrature to a systematic error of 6.5%. The total systematic error excluding  $b \rightarrow u$  and  $b \rightarrow c$  model dependences amounts to 18%.

## SUMMARY

In summary, the relative partial branching fraction for  $B \rightarrow X_u \ell \nu$  decays in the kinematic region  $M_X < 1.7 \text{ GeV}/c^2$ ,  $q^2 > 8 \text{ GeV}^2/c^2$  is

$$\frac{\Delta\mathcal{B}(B \rightarrow X_u \ell \nu)}{\mathcal{B}(B \rightarrow X \ell \nu)} = [0.92 \pm 0.14(\text{stat}) \pm 0.17(\text{syst}) \pm 0.04(b \rightarrow u) \pm 0.06(b \rightarrow c)] \times 10^{-2} \quad , \quad (2)$$

where the first error is statistical, the second experimental systematic, and the third and fourth arise from uncertainties in modeling the  $B \rightarrow X_u \ell \nu$  and  $B \rightarrow X_c \ell \nu$  transitions. By using the measured semileptonic branching fraction  $\mathcal{B}(B \rightarrow X \ell \nu) = 0.1073 \pm 0.0028$  [16], we obtain

$$\Delta\mathcal{B}(B \rightarrow X_u \ell \nu) = [0.99 \pm 0.15(\text{stat}) \pm 0.18(\text{syst}) \pm 0.04(b \rightarrow u) \pm 0.07(b \rightarrow c)] \times 10^{-3} \quad . \quad (3)$$

The branching fraction  $\mathcal{B}(B \rightarrow X_u \ell \nu)$  is calculated from the above value through the expression

$$\mathcal{B}(B \rightarrow X_u \ell \nu) = \Delta\mathcal{B}(B \rightarrow X_u \ell \nu)/f_u \quad . \quad (4)$$

The extrapolation coefficient  $f_u$  is estimated to be  $0.303 \pm 0.035$  using the De Fazio and Neubert (FN) prescription [10] with the  $b$ -quark shape function parameters  $m_b = 4.62 \text{ GeV}/c^2$  and  $\mu_\pi^2 = 0.40 \text{ GeV}^2/c^2$  and their one sigma error ellipse, which are determined from a recent Belle  $B \rightarrow X_s \gamma$  measurement [12, 17]. It is rescaled to  $0.294 \pm 0.035$  by multiplying by a factor  $f_{u0}(\text{BLL})/f_{u0}(\text{FN}) = 0.324/0.334$ , where  $f_{u0}(\text{BLL})$  and  $f_{u0}(\text{FN})$  denote the  $f_u$  values calculated for the values of  $m_b = 4.71 \text{ GeV}/c^2$  and  $\mu_\pi^2 = 0.2 \text{ GeV}^2/c^2$  by the Bauer, Ligeti and Luke (BLL) [2] and De Fazio and Neubert prescriptions, respectively. In both  $\alpha_s$  and  $1/m_b$  expansions the BLL prescription contains corrections of higher order than the FN prescription. The uncertainty of  $f_u$  is modified by including the contributions from the subleading shape function and the weak annihilation. The former is estimated to be 4% [18] and the latter is estimated to be 8% [2]. As a result we use  $f_u = 0.294 \pm 0.044$  in Eq.(4). This yields

$$\mathcal{B}(B \rightarrow X_u \ell \nu) = [3.37 \pm 0.50(\text{stat}) \pm 0.60(\text{syst}) \pm 0.14(b \rightarrow u) \pm 0.24(b \rightarrow c) \pm 0.50(f_u \text{ error})] \times 10^{-3} \quad , \quad (5)$$

where the additional error comes from the uncertainty in the calculation of  $f_u$ .

Combining this result with the average  $B$  lifetime  $\tau_B = (1.587 \pm 0.011) \text{ ps}$  [16], the CKM matrix element  $|V_{ub}|$  is obtained by using the formula

$$|V_{ub}| = 0.00424 \left( \frac{\mathcal{B}(B \rightarrow X_u \ell \nu)}{0.002} \frac{1.61 \text{ ps}}{\tau_B} \right)^{1/2} \quad , \quad (6)$$

which is an updated version of the expression given in [19], and incorporates the latest measurements of the heavy-quark parameters [20]. Finally, we obtain

$$|V_{ub}| = [5.54 \pm 0.42(\text{stat}) \pm 0.50(\text{syst}) \pm 0.12(b \rightarrow u) \pm 0.19(b \rightarrow c) \pm 0.42(f_u \text{ error}) \pm 0.27(\mathcal{B} \rightarrow |V_{ub}| \text{ error})] \times 10^{-3} \quad . \quad (7)$$

The first four errors are statistical, systematic,  $b \rightarrow c$  and  $b \rightarrow u$  model dependence. The latter two are due to uncertainties of  $f_u$  and of the relation between  $\mathcal{B}$  and  $|V_{ub}|$  in Eq. (6), respectively.

The present work demonstrates the effectiveness of  $M_X$  and  $q^2$  measurements of  $B \rightarrow X_u \ell \nu$  decays using full reconstruction tagging. The result is consistent with previous measurements of  $\mathcal{B}(B \rightarrow X_u \ell \nu)$  [1, 3, 4, 21]. In the future, further accumulation of data as well as MC data will allow us to reduce the statistical error, and better understanding of the signal and the background components will help to improve the experimental systematics as well as constrain the theoretical uncertainties.

We thank the KEKB group for the excellent operation of the accelerator, the KEK Cryogenics group for the efficient operation of the solenoid, and the KEK computer group and the National Institute of Informatics for valuable computing and Super-SINET network support. We acknowledge support from the Ministry of Education, Culture, Sports, Science, and Technology of Japan and the Japan Society for the Promotion of Science; the Australian Research Council and the Australian Department of Education, Science and Training; the National Science Foundation of China under contract No. 10175071; the Department of Science and Technology of India; the BK21 program of the Ministry of Education of Korea and the CHEP SRC program of the Korea Science and Engineering Foundation; the Polish State Committee for Scientific Research under contract No. 2P03B 01324; the Ministry of Science and Technology of the Russian Federation; the Ministry of Education, Science and Sport of the Republic of Slovenia; the National Science Council and the Ministry of Education of Taiwan; and the U.S. Department of Energy.

---

\* on leave from Nova Gorica Polytechnic, Nova Gorica

- [1] B. Aubert *et al.* (BaBar Collaboration), Phys. Rev. Lett. **92**, 071802 (2004).
- [2] C. W. Bauer, Z. Ligeti and M. E. Luke, Phys. Rev. **D 64**, 113004 (2001).
- [3] H. Kakuno *et al.* (Belle Collaboration), Phys. Rev. Lett. **92**, 101801 (2004).
- [4] R. Fulton *et al.* (CLEO Collaboration), Phys. Rev. Lett. **64** 16 (1990), J. Bartelt *et al.* (CLEO Collaboration), Phys. Rev. Lett. **71**, 4111 (1993), A. Bornheim *et al.* (CLEO Collaboration), Phys. Rev. Lett. **88**, 231803 (2002); H. Albrecht *et al.* (ARGUS Collaboration), Phys. Lett. **B 234**, 409 (1990); B. Aubert *et al.* (BaBar Collaboration), arXiv:hep-ex/0207081, K. Abe *et al.* (Belle Collaboration), BELLE-CONF-0325.
- [5] S. Kurokawa and E. Kikutani, Nucl. Instr. and Meth. **A499**, 1 (2003), and other papers included in this Volume.
- [6] A. Abashian *et al.* (Belle Collaboration), Nucl. Instr. and Meth. **A479**, 117 (2002).
- [7] R. Brun, F. Bruyant, M. Maire, A. C. McPherson and P. Zanarini, CERN Report No. DD/EE/84-1 (1984).
- [8] P. Ball, arXiv:hep-ph/0306251.
- [9] D. Scora and N. Isgur, Phys. Rev. **D 52**, 2783 (1995).
- [10] F. De Fazio and M. Neubert, J. High Energy Phys. **9906**, 017 (1999).
- [11] QQ  $B$  meson event generator, developed by the CLEO Collaboration, <http://www.lns.cornell.edu/public/CLEO/soft/QQ>.
- [12] A. Limosani and T. Nozaki (Belle Collaboration), hep-ex/0407052.
- [13] G. C. Fox and S. Wolfram, Phys. Rev. Lett. **41**, 1581 (1978).
- [14] J.E. Gaiser *et al.*, Phys. Rev. **D 34**, 711 (1986).
- [15] H. Albrecht *et al.* (ARGUS Collaboration), Z. Phys. **C 48**, 543 (1990).
- [16] S. Eidelman *et al.*, Phys. Lett. **B592**, 1 (2004).

- [17] P. Koppenburg *et al.* (Belle Collaboration), Phys. Rev. Lett. **93**, 061803 (2004).
- [18] <http://www.slac.stanford.edu/xorg/hfag/semi/winter04/writeup.ps>
- [19] K. Hagiwara *et al.*, Phys. Rev. **D66**, 010001 (2002).
- [20] B. Aubert *et al.* (BaBar Collaboration), Phys. Rev. Lett. **93**, 011803 (2004)
- [21] R. Barate *et al.* (ALEPH Collaboration), Eur. Phys. J. **C 6**, 555 (1999); M. Acciarri *et al.* (L3 Collaboration), Phys. Lett. **B 436** 174 (1998); P. Abreu *et al.* (DELPHI Collaboration), Phys. Lett. **B 478** 14 (2000); G. Abbiendi *et al.* (OPAL Collaboration), Eur. Phys. J. **C 21**, 399 (2001); A. Bornheim *et al.* (CLEO Collaboration), CLEO-CONF 02-08.